Importin-β: Structural and Dynamic Determinants of a Molecular Spring

Ulrich Zachariae[1,*] and Helmut Grubmüller[1]
[1]Max Planck Institute for Biophysical Chemistry, Am Fassberg 11, 37077 Göttingen, Germany
*Correspondence: uzachar@gwdg.de

SUMMARY

The β-karyopherin/RanGTP system constitutes the largest known family of cellular cargo transporters. The flexibility of the karyopherin transport receptors is the key to their versatility in binding cargoes of different shape and size. Despite strong binding of the Ran complex, the comparably low energy associated with GTP hydrolysis suffices to drive dissociation and fuel the transport cycle. Here, we elucidate the drastic structural dynamics of the prototypic karyopherin, importin-β, and show that its flexibility also solves this energetic puzzle. Our nonequilibrium atomistic simulations reveal fast conformational changes, validated by small-angle X-ray scattering data, and unusually large structural fluctuations. The characteristic dynamic patterns of importin-β and the observed unfolding pathway of the IBB domain suggest a cooperative mechanism of importin-β function in the nucleus. We propose a molecular model in which the stored energy and structural dynamics account for an exchange pathway that explains the high observed rates of nucleocytoplasmic transport. Karyopherins utilize a mechanism of entropy/enthalpy control that might be a general feature of highly flexible proteins involved in protein-protein interactions.

INTRODUCTION

Receptor-mediated transport of proteins and RNA between the cell nucleus and the cytoplasm via nuclear pore complexes (NPCs) is essential for the control and exchange of genetic information in eukaryotes (Cook et al., 2007; Stewart, 2007; Weis, 2003; Fahrenkrog and Aebi, 2003). The largest evolutionarily conserved family of nuclear transport receptors is the β-karyopherin family, named after their prototype, importin-β (Cook et al., 2007; Mosammaparast and Pemberton, 2004). Aside from its function in nucleocytoplasmic transport, importin-β was recently recognized as a global regulator of transport-related cellular functions in the cell cycle, such as centrosome dynamics, mitotic spindle assembly, and the insertion of integral membrane proteins into the inner nuclear membrane (Harel and Forbes, 2004; King et al., 2006). Importin-β also probably acts as a chaperone for highly basic proteins in the cytoplasm

(Jäkel et al., 2002). In all of its roles, importin-β interacts with the GTP-bound form of the small G protein Ran as an effector switching importin-β between cargo uptake and release (Figure 1A). The high specificity and stability of cargo and Ran complexes requires the observed strong binding to importin-β, which, however, seems incompatible with the measured high exchange rates, especially during nucleocytoplasmic transport (Görlich et al., 2003; Ribbeck and Görlich, 2001). Unusually high flexibility was inferred from the crystal structures showing different conformations bound to cargo proteins, RanGTP, or nucleoporins (Lee et al., 2000, 2003, 2005; Liu and Stewart, 2005; Fukuhara et al., 2004; Vetter et al., 1999; Cingolani et al., 1999). The stacking of 19 HEAT repeats in importin-β, each formed by a hairpin of two α helices and a short loop (Cook et al., 2007; Conti et al., 2006), creates a superhelical structure built from modular folding units (Figures 1B and 1C). In similar structures, the lack of a sizable globular hydrophobic core has been found to be probably responsible for enhanced conformational freedom (Sotomayor and Schulten, 2007). In addition, in importin-β, the hydrophobic core is extended along the superhelix.

To elucidate the thermodynamic and kinetic puzzles of nucleocytoplasmic transport, knowledge of the structure and the energetics of the unbound state of importin-β is essential. However, neither the unbound structure nor its dynamics have been accessible so far, except for small-angle X-ray scattering (SAXS) measurements (Fukuhara et al., 2004). The SAXS data indicate a substantially extended structure of unbound importin-β (the radius of gyration [R_G] is increased by ∼1 nm), which implies that importin-β undergoes a large conformational motion between its bound, compact state and the extended free form. Because of its remarkable abundance in the cytoplasm (Jäkel et al., 2002), the free state of importin-β is assumed to play an important biological role in addition to binding cargo for transport between the cytoplasm and the nucleus. Here, we elucidate the structure and dynamics of the free state of importin-β in solution and the mechanisms underlying its interactions with RanGTP and cargo by nonequilibrium and equilibrium molecular dynamics (MD) simulations, validated by the experimental data (Fukuhara et al., 2004).

RESULTS

The Unbound State of Importin-β

We have aimed at predicting both the unbound structure of importin-β in solution and its fluctuations. First, we removed RanGTP from the yeast importin-β complex (Lee et al., 2005;
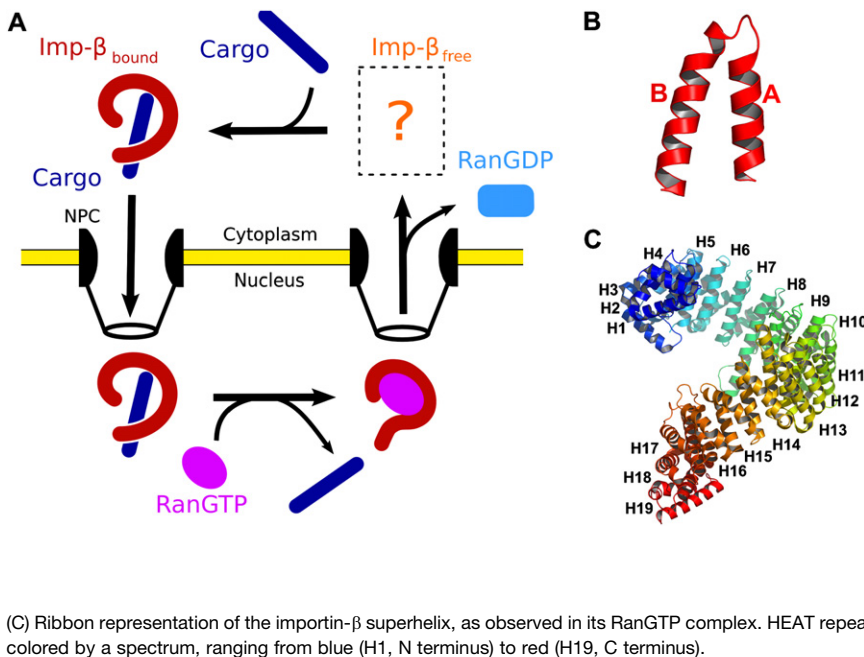
Figure 1. Importin-β-Mediated Nuclear Import Cycle

(A) Importin-β's best-characterized function is the nuclear import of cargo proteins tagged with a classical nuclear localization signal (NLS), which are bound by importin-β in the cytoplasm involving the adaptor protein importin-α. Some cargoes can also directly associate with the receptor. Importin-β encloses its cargo or the importin-β binding domain of importin-α (IBB, blue) for translocation. After transfer through the NPC, RanGTP (magenta) binds to importin-β, and drives rapid cargo release. The importin-β-RanGTP complex subsequently travels back to the cytoplasm, where it is disassembled. Hydrolysis of RanGTP to RanGDP (light blue) in the cytoplasm renders disassembly irreversible. The atomic structure of the unbound state of importin-β is unknown, representing a missing link in the cycle.

(B) HEAT repeat, formed by a hairpin of α helices ("A" and "B") and a loop. The A helices form the external, convex surface of importin-β interacting with the NPC, while the B helices provide the binding sites for cargo and RanGTP on the internal surface of importin-β.

(C) Ribbon representation of the importin-β superhelix, as observed in its RanGTP complex. HEAT repeat numbers are given as H1–H19 and HEAT repeats are colored by a spectrum, ranging from blue (H1, N terminus) to red (H19, C terminus).

Figure 2A) to determine whether the conformation adopted by importin-β in the complex is stable. Freed importin-β underwent an extremely rapid and extensive opening motion in our simulations, increasing the end-to-end distance from 8.6 nm to 14.8 nm already within ~24 ns. To our knowledge, this is the fastest and largest protein conformational change observed in MD simulations so far. Measured in terms of the protein's R_G, the size of importin-β rose from 3.6 nm to up to ~4.6 nm (Figure 2B), in agreement with the SAXS data (Fukuhara et al., 2004). After this fast opening, the free form of importin-β in solution formed a highly flexible S-like extended structure. Its average end-to-end length was ~14 nm, and its helicoidal pitch was ~12 nm (increased from ~6 nm). The measured R_G of 4.6 ± 0.1 nm (Fukuhara et al., 2004), corrected for the contribution from the protein's hydration shell (typically ~0.3 nm; Svergun et al., 1998), is in excellent agreement with our prediction. We observed the tight helical character to be almost completely lost in the transition, and comparably fast expansions from the compact state were reproduced in several simulations (see below).

For comparison, we also simulated the RanGTP complex. While the free structure showed large fluctuations around an average R_G of ~4.4 nm (Figure 2B, red curve), the RanGTP-bound complex remained very close to the compact crystal structure, with an R_G of ~3.5 nm (Figure 2B, black curve).

We have validated the atomic structure obtained from the simulation against the available low-resolution SAXS data of free importin-β in solution (Fukuhara et al., 2004). Aside from the excellent agreement of the R_G, our predicted atomic structure fully agrees with the low-resolution density obtained from the SAXS data (Fukuhara et al., 2004; Figure 2C), with a very high statistical significance of ~10^{-4}% (see Figure S1 in the Supplemental Data available with this article online). In addition, with a similar approach, we have recently successfully predicted the crystal structure of cytoplasmic exportin Cse1p with a root-mean-square deviation (rmsd) of 3 Å (Zachariae and Grubmüller, 2006).

Transition to the Extended State and Regions of Flexibility

Next, we analyzed the dynamics of the fast opening motion of importin-β. As shown in Figure 2B, the large conformational change occurred in two phases. In the initial expansion, the R_G abruptly increased from 3.6 nm to 4.1 nm within only ~2 ns (Figure 2B), corresponding to a $C_α$ rmsd of ~0.8 nm. It comprised a significant loss of curvature between the RanGTP binding sites at HEAT repeats 1–3 and 12–15. The distance between HEAT repeat 1 and HEAT repeat 13 increased from 2.7 nm to ~4.5 nm ($C_α$ atoms of Asp18 and Thr562 were taken as reference). The opening was accompanied by a rise in helicoidal pitch from ~6 nm to ~8.5 nm that vigorously drove both termini apart (Figure 2E). This rapid first transition can be attributed to an accumulation of small structural changes within and between HEAT repeats, while their internal structure changed only slightly. The angles between successive HEAT repeats varied only by up to 15°, and the rmsd of individual HEAT repeats remained in the range of ~0.2 nm, while the accumulation of these effects led to an enormous structural change. During the second phase, expansion continued on a slower time scale, and, here, clear differences between and within HEAT repeats emerged (Figure S2). The R_G reached values of ~4.2–4.6 nm (maximum $C_α$ rmsd ~2 nm), and underwent large fluctuations (Figure 2B).

According to their dynamics, three different regions can be distinguished in the structure of importin-β: the flexible N-terminal HEAT repeats 1–5, a region of relatively high rigidity between HEAT repeats 6 and 13, and the flexible HEAT repeats 14–19. On top of the incremental relaxation of the HEAT repeats, two main hinge motions dominated the conformational relaxation during the second regime (Figure 3 and Figure S2). The central section showed only few changes, while HEAT repeats 4 and 5 in the N-terminal section and HEAT repeats 14–15 in the C-terminal section formed dynamic "hotspots". In helix 5B, the angle of the kink, formed at Ser208 (Ser201 in human importin-β), increased
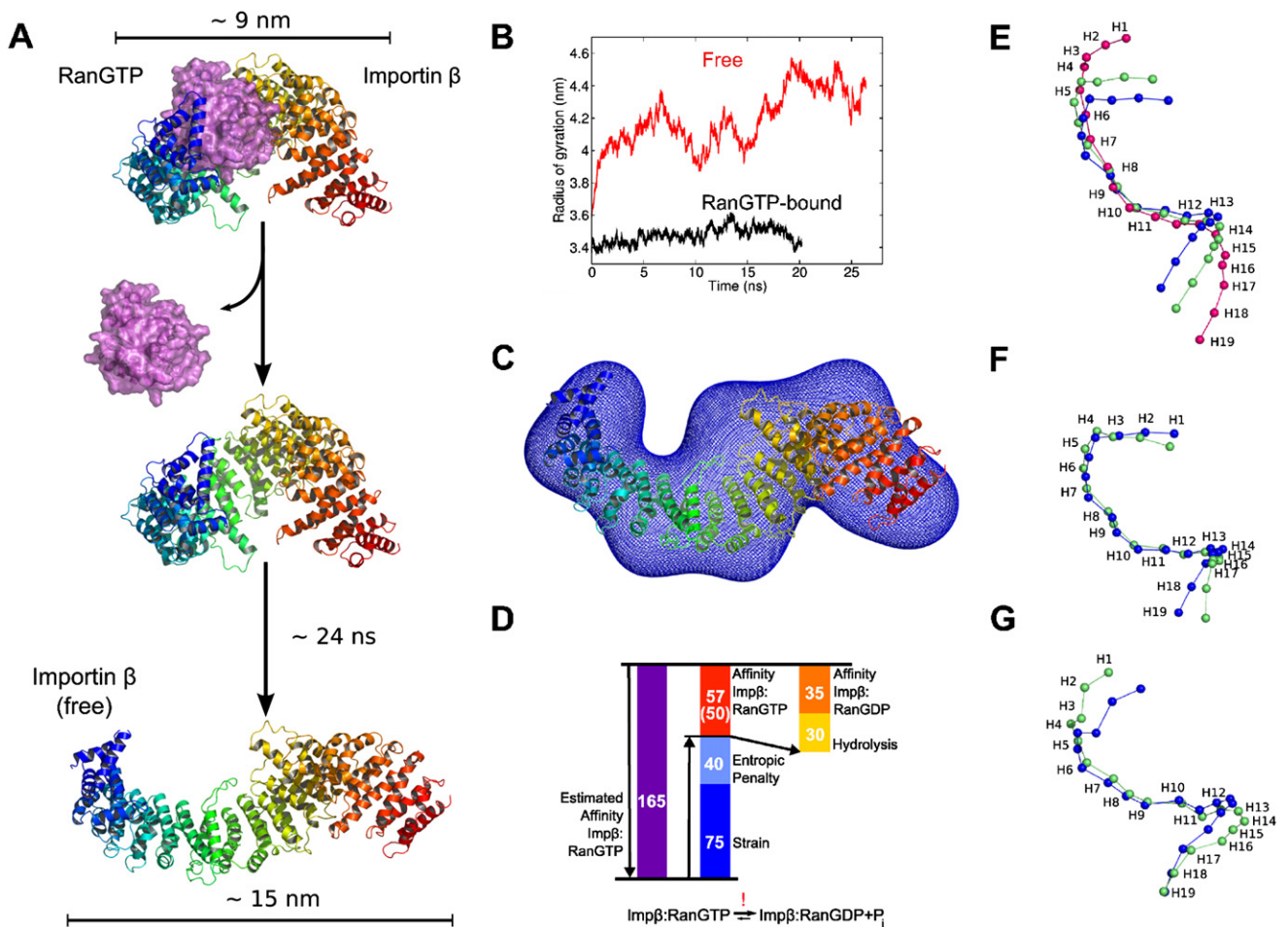
Figure 2. Importin-β Undergoes a Dramatic Conformational Change

(A) RanGTP (magenta) was removed from the structure of full-length importin-β. A rapid and extensive conformational change followed in the simulation. The structure of importin-β is shown in a cartoon representation, colored in a spectrum from blue (N terminus) to red (C terminus).

(B) R_G of dissociated importin-β (red curve) and of RanGTP-bound importin-β (black curve). The gyration radius increased from ~3.6 nm to ~4.2–4.6 nm in the dissociated state, while it remained near ~3.5 nm in the complex. The extension of free importin-β exhibits a very fast initial phase and a slower subsequent expansion.

(C) Average final atomic structure of free importin-β obtained from our MD simulations (cartoon representation) compared to the small-angle X-ray scattering model of free importin-β in solution (blue mesh).

(D) Fine tuning of free energy in the importin-β-RanGTP complex. Strain (dark blue bar) and entropic restriction (light blue bar) reduce the estimated affinity resulting from the very large interaction surface from ~165 kJ/mol (purple) to a measured value of 57 kJ/mol (estimated value, ~50 kJ/mol; red). To thermodynamically enable GTP hydrolysis to drive dissociation, this value has to be lower than the sum of the affinity of importin-β to RanGDP (orange; ~35 kJ/mol) and the free energy obtainable from GTP hydrolysis in the standard state (yellow; ~30 kJ/mol).

(E–G) Overall flexibility of the HEAT repeat scaffold shown as maximum deviation of HEAT repeat centers from their original positions. The location of the center of each HEAT repeat (H1–H19) is shown as a sphere. (E) Simulation of importin-β dissociated from the RanGTP complex. (F) Simulation of importin-β in the RanGTP-bound form. (G) Simulation of the cargo complexes of importin-β (the SREBP-2-bound state is shown here).

from 55° to 85°; simultaneously, the distance between helices 5A and 5B rose by 0.3 nm. The hinge is located at a conserved LXFX motif here, the bending of which affected the entire N-terminus and increased the diameter of the arch between HEAT repeat 1 and 13 further, to ~6 nm. At the C terminus, a conserved FXKY motif in the loop between helices 14B and 15A formed a hinge, which underwent strong bending. A proline kink in helix 15B (residue 642; residue 653 in human importin-β) transmitted this motion in a domino-like fashion on to the C terminus. This led to a significant shift of the centers of HEAT repeats 15–19 from their original positions. No hinges were observed in the central region

between HEAT repeats 6 and 13. These observations are in good agreement with the conclusions drawn by Cansizoglu and Chook (2007) and by Lee et al. (2005) from comparison of crystal structures of transportin or importin-β, respectively. However, they raise questions about the notion of karyopherins being composed of two arches of HEAT repeats connected by only one major hinge in the center (Chook and Blobel, 2001; Conti et al., 2006).

RanGTP Renders Importin-β Rigid

To assess how bound RanGTP (Lee et al., 2005) alters the dynamics and flexibility of importin-β, we performed additional
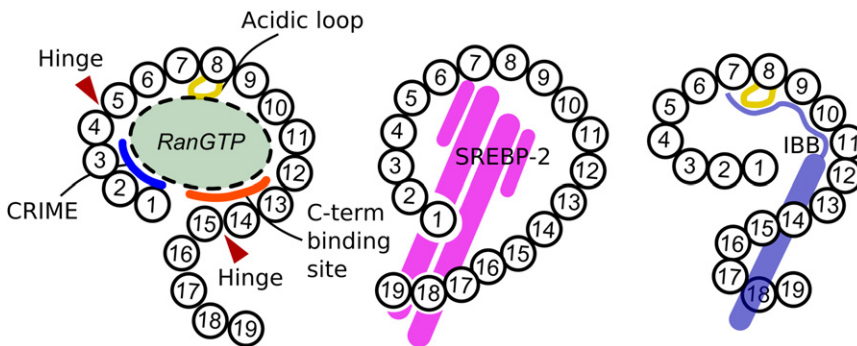
Figure 3. Schematic Drawing of the Binding Modes of Importin-β to RanGTP, SREBP-2, and the IBB Domain

RanGTP is bound via the N-terminal CRIME region, an area around the acidic loop 8, and an extended, more C-terminal binding site. SREBP-2 is gripped between HEAT repeats 7 and 17, while the IBB domain binds to an extended region between HEAT repeats 7 and 19, involving, in particular, the acidic loop at HEAT repeat 8.

simulations of the complex. Figure 2F shows that the positions of the first 17 HEAT repeats are essentially unchanged with respect to the crystal structure. RanGTP constituted the least flexible part of the complex (Figure S3) and formed a core of stability for the first 15 HEAT repeats of importin-β, to which it is tightly bound. Moreover, by locking the hinge between HEAT repeats 14 and 15, the C terminus was stiffened. Only the far C-terminal section of importin-β, not involved in Ran binding (HEAT repeats 17–19), exhibited larger fluctuations. This result is consistent with and specifies the molecular basis for the previous suggestion that RanGTP binding imposes a specific curvature on the C terminus that is incompatible with cargo rebinding (Lee et al., 2005).

The observed residual dynamics of importin-β in the RanGTP-bound state were much smaller in amplitude than the dynamics of the free state, and the average rmsd of the RanGTP-bound form remained as low as 0.25–0.37 nm. In contrast, the dissociated form exhibited an average rmsd of ~1.45 nm in phase two of the transition. We suggest that the salt-bridging triad of Lys27 (Ran), Glu615 (Imp-β, HEAT repeat 14), Lys646 (Imp-β, HEAT repeat 15), and the additional hydrogen bond between Lys27 (Ran) and Gln650 (Imp-β, HEAT repeat 15) contribute significantly to the inhibition of the hinge at HEAT repeats 14 and 15 in the RanGTP-bound state by interlocking it. The switch function of HEAT repeats 14 and 15 is consistent with experimental findings in which the Ran mutant K27D/K152A showed hindered cargo replacement upon binding to importin-β. This was attributed to its inability to impose a specific curvature on the C terminus that is incompatible with cargo binding (Lee et al., 2005).

Fine-Tuned Energetics

In addition to its remarkable conformational dynamics, the reaction cycle of importin-β raises intriguing questions concerning its energetics and kinetics. In particular, importin-β binds RanGTP via a very large interaction surface to ensure highly specific recognition and to displace cargo from different binding sites. This leads to the expectation of exceedingly high binding energies (Lee et al., 2005; Conti et al., 2006). Despite very stable binding of RanGTP to importin-β (Kutay et al., 1997), however, the relatively small energy released by GTP hydrolysis to GDP is sufficient to drive rapid complex dissociation (Lee et al., 2005; Kutay et al., 1997). In fact, the dissociation rates support an impressively high measured overall rate of nuclear transport of up to 10^3 translocation events per second per NPC (Ribbeck and Görlich, 2001). An intriguing aspect of this paradox comes from the recent determination of the structure of the complex formed by

full-length importin-β and RanGTP, which revealed three major regions of contact between the transport receptor and its effector (Lee et al., 2005). It was found previously that fragments of importin-β comprising only residues 1–462 (i.e., the first two binding sites) show almost the same affinity to RanGTP as the full-length protein (Kutay et al., 1997). The third binding site, however, additionally buries a large amount of hydrophobic surface, and yields at least three H bonds and two salt bridges, such that a substantial gain in affinity should be expected. To account for the missing free energy, it was proposed that importin-β stores a large amount of energy internally, either by significant mechanical distortion or via enthalpy-entropy compensation (Lee et al., 2005; Conti et al., 2006). Our simulations allowed us to address this issue.

Indeed, the fast and irreversible opening motion against considerable Stokes friction that we observed for free importin-β points to substantial strain. In addition, the enhanced flexibility seen for the free state implies a significant entropy. From the longest trajectory (~27 ns), we estimated the major energy contributions.

Through friction, we estimated that the rapid expansion of the protein dissipated a maximum free energy on the order of ~75 kJ/mol to the solvent. The difference in the protein's conformational entropy in the bound and free states was estimated to be on the order of ~40 kJ/mol. Accordingly, both the mechanical distortion of the complexed structure and the restricted entropy of the complex combine to form a highly loaded spring. From our estimate, the mechanical distortion contributes about twice as much to the stored free energy as the loss of entropy.

The large total amount of estimated stored free energy (~115 kJ/mol) resolves the paradox of achieving high binding specificity under the preservation of reversibility (Figure 2D). The RanGTP complex buries ~1200 Å^2 of hydrophobic surface area. Although, in many cases, the amount of buried surface area is not directly commensurate with complex stability, trends can be established (Eisenberg and McLachlan, 1986; Vallone et al., 1998). By taking an average value for the enhancement of stability upon burial of hydrophobic surface area (Vallone et al., 1998), we estimated a contribution of about 75 kJ/mol to thermodynamic stability in the RanGTP complex. In addition, the interface exhibits a strong polar and electrostatic contribution from seven H-bonding contacts (~7 kJ/mol each; Pace et al., 1996), and at least seven salt bridges (on average, ~6 kJ/mol each; Schreiber and Fersht, 1995). We thus estimated the lower limit of the binding free energy of RanGTP to importin-β to be ~165 kJ/mol (Figure 2D, purple bar). This value would

render dissociation of the complex practically impossible. However, fast dissociation rates are implied by the high turnover numbers involved in nuclear transport. The stored free energy estimated above (Figure 2D, dark/light blue bars) would decrease the affinity of the RanGTP complex to about 50 kJ/mol (red). We note that this energy may be overestimated by our nonequilibrium method, because, due to possibly insufficient sampling, the result cannot be corrected for slow equilibrium fluctuations, which, per definition, are not driven by free energy differences.

With respect to cargo and RanGTP exchange kinetics, we suggest that the high turnover rates are at least partly supported by release of the stored energy during relaxation of the importin-β spring. An intimate interplay between the dynamics of importin-β, and the rate-enhancing effects of RanBP1 and importin-α (in the cytoplasm), as well as those of nucleoporins (Nup1/Nup2), Cse1, and importin-α (in the nucleus), is conceivable. We suggest that cooperative exchange mechanisms may play a crucial role here (see Discussion).

With regard to the thermodynamics of the system, it is critical that the difference in affinities of importin-β toward RanGTP (Figure 2D, red bar) and RanGDP (orange bar) does not exceed the free energy obtainable from GTP hydrolysis (Goody, 2003) (~30 kJ/mol, yellow bar). In that case, the equilibrium would be shifted to importin-β-bound RanGTP, and the RanGTP-bound form would be spontaneously restored from the RanGDP complex and cellular inorganic phosphate. The system would thus turn itself on, and become stuck in the RanGTP-bound state. The affinity of RanGDP toward importin-β was measured to be ~35 kJ/mol (Vetter et al., 1999). The high strain put into importin-β in the RanGTP-bound state reduces the affinity of RanGTP to importin-β to a measured value of ~57 kJ/mol (Bischoff and Görlich, 1999; Villa Braslavsky et al., 2000; Figure 2D, red bar). We suggest that this fine tuning of free energies with strain and an entropic penalty, as shown in our simulations, prevents GTP blockade of the cycle, despite high RanGTP binding specificity, and thus forms the basis for RanGTP control of the various functions of importin-β.

The Dynamics of the Cargo-Bound States of Importin-β

Aside from their thermodynamic basis, the high observed rates of nuclear transport raise important questions on the kinetics of the involved transitions. All importin-β-cargo complexes exhibit high stability (the affinity of the IBB domain to importin-β is ~0.6 nM) (Koerner et al., 2003). Thus, the transition from the cargo-bound form to the RanGTP-bound state should be very slow based on passive dissociation, unless a cooperative mechanism is involved that drastically reduces the dissociation barrier. We simulated both importin-β bound to the IBB domain of importin-α (Cingolani et al., 1999) as well as to the nonclassical nuclear localization signal cargo fragment sterol regulatory element binding protein (SREBP)-2 (Lee et al., 2003). Importin-β binds the IBB via an extended surface between the acidic loop at HEAT repeats 8 and 19, while SREBP-2 is gripped by the extended HEAT repeats 7 and 17.

We analyzed the dynamics of both cargo complexes in the context of the allosteric model of importin-β cargo exchange, proposed by Lee et al. (2005). Compared to the open state, both complexes exhibited decreased flexibility, but were slightly
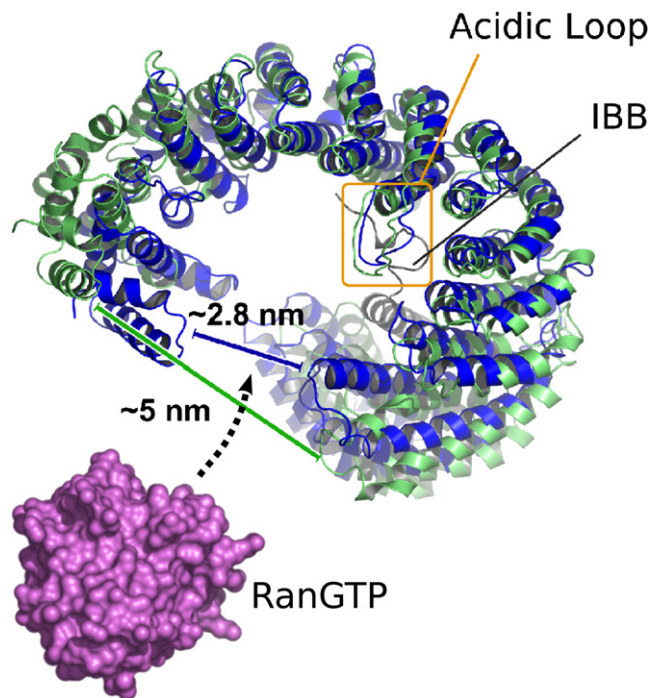

Figure 4. Opening of the N-Terminal Segment of Importin-β
Cargo-bound structures open up their N-terminal regions. The region comprising HEAT repeats 1–13 of the crystal structure of importin-β (blue) bound to the IBB domain of importin-α (IBB, gray) is shown in comparison with a representative snapshot from the MD simulation (green). The distances illustrating the opening of the N-terminal arch are shown. For size comparison, the RanGTP protein, which enters the arch, is drawn in surface representation (magenta). The acidic loop of importin-β (yellow box) exhibits moderate fluctuation in the bound state.

less rigid than the RanGTP-bound state (average rmsds bound to IBB or SREBP-2, 0.47 nm). In particular, the presence of both cargo structures rigidified the C-terminal end of importin-β (Figures S2 and S3). In contrast, the N terminus opened up and exhibited strong fluctuations. In both cases, HEAT repeats 1–3 formed the most flexible region, and the section between HEAT repeats 13–16 constituted a second region of flexibility (Figure 2G). The hinge between HEAT repeats 4 and 5 was partially inhibited by bound cargo. Despite their fundamentally different binding modes to importin-β, both cargoes impose nearly identical fluctuation patterns (Figure S3). The inherent flexibility increased the distance of the arch formed between the Ran binding sites at HEAT repeats 1–4 and 13–14 from ~2.8 nm to ~5.0 nm (IBB; Figure 4) and ~5.4 nm (SREBP-2; the Cα positions of Glu 19 and Thr 571 were taken as reference).

We suggest that the large opening motion of the N terminus of importin-β is essential for rapid entry of the large RanGTP protein into the tightly wound cargo-bound structure of importin-β in the nucleus (Figure 4). The enhanced dynamics of the importin-β N terminus thus serves to lower the dissociation barrier and increase exchange rates by allowing for a cooperative exchange mechanism. Here, the IBB domain is not required to passively dissociate before the RanGTP protein can enter the importin-β superhelix, and then actively displaces the IBB from its N-terminal binding sites. Such a cooperative mechanism is
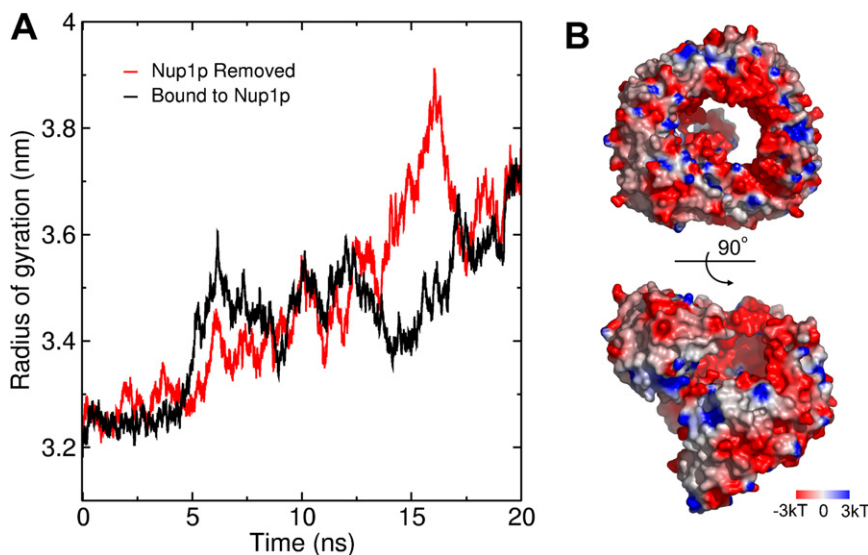
Figure 5. Nup1p-Bound Importin-β Expands Spontaneously

(A) The importin-β conformation observed in the Nup1p-bound structure undergoes rapid extensions, both when the fragment of Nup1p determined in the crystal structure is removed (red curve) and when it remains bound.

(B) Electrostatic surface potential of Kap95p (red, negative; blue, positive). The inner surface of Kap95p is highly negative due to a large surplus of acidic residues. It forms a negatively charged channel (e.g., for the highly basic, bound IBB domain), but leads to an instable electrostatic configuration in a compact unbound state.

further supported by the dynamic behavior of the IBB domain upon dissociation (see below). We note that, in simulations in which cargo was removed from the compact importin-β structure, importin-β showed a rapid biphasic expansion similar to the cases in which RanGTP was removed from importin-β (Figure S4). This suggests that both the IBB domain and SREBP-2 load the importin-β spring by connecting the flexible C terminus with the rigid region comprising HEAT repeats 6–13.

Importin-β Bound to Nup1p

We next examined yeast importin-β (Kap95p) bound to and freed from the nucleoporin Nup1p (Liu and Stewart, 2005). As nucleoporins mainly bind to the external surface of importin-β, and, thereby, cannot easily connect the two flexible ends, their effect on the structure of importin-β should be relatively small. In the crystal structure of the complex, a short fragment of Nup1p (residues 963–1076) is seen to be bound between the external A helices of HEAT repeats 5–8 of Kap95p. Binding is mediated by a number of phenylalanine residues from Nup1p buried in hydrophobic grooves on the surface of Kap95p. The static crystal structure of Kap95p is very compact with an R_G of only ∼3.15 nm. The geometry adopted by the transport receptor is very similar to the IBB-bound conformation, and two intramolecular contacts are formed between the N terminus and the C terminus of Kap95p (Liu and Stewart, 2005).

The Nup1p-bound structure is thought to likely represent an approximation of the unbound state, because the stretch of Nup1p clearly seen in the crystal structure is rather short. However, the crystal structure does not account for the role of the last 60 residues of Nup1p, which clearly increase the affinity for Kap95p. This stretch contains numerous basic residues (Liu and Stewart, 2005; Pyhtila and Rexach, 2003). It is most likely that these residues partially mimic those of the importin-α IBB domain and bind inside its binding channel (Liu and Stewart, 2005). Our simulation system exclusively contained residues that are assigned in the crystal structure (i.e., these C-terminal 60 Nup1p residues were not modeled). In one simulation, the visible Nup1p fragment bound to the external surface was also removed.

In our simulations, the conformation of yeast importin-β bound to Nup1p, as reported in the crystal structure (Liu and Stewart, 2005), was not observed to be stable (Figure 5). The contacts between HEAT repeats 2/4–17, and repeats 7–18/19 were lost relatively soon in both simulations. Subsequently, the import receptors expanded vigorously as their flexible termini became disconnected from each other, regardless of whether the remaining Nup1p fragment was bound at the outside or not (Figure 5). This observation suggests that importin-β spontaneously assumes an extended state in solution, unless either cargo or RanGTP is bound to the inner surface.

We speculate that the unassigned section of Nup1p is either bound, but not seen, inside importin-β in the crystal structure, keeping its termini together, or that crystal constraints act in favor of a compacted shape of Kap95p. In the crystal structure, extensive contacts are made between the basic external surface of HEAT repeats 18 and 19 and the acidic internal binding channel formed by all HEAT repeats in the neighboring molecule. If the last 60 residues of Nup1p were indeed bound inside the cargo binding channel, this might suggest that Nup1p plays an active role in dissociating cargo from importin-β in the nucleus by competition. Nup1p is asymmetrically localized to the nuclear basket of the NPC and binds importin-β with a substantially higher affinity than other nucleoporins (Pyhtila and Rexach, 2003).

The IBB Domain Rapidly Unfolds upon Dissociation from Importin-β

We examined the stability of the IBB domain of importin-α in its α-helical form, which it adopts bound to importin-β (residues 11–54) in extended MD simulations. The IBB domain is highly positively charged, with 16 basic groups and only 6 acidic residues present in this section.

The helix was seen to unfold almost completely within ∼48 ns (Figure 6A). In contrast, the helicity of the IBB domain was completely preserved within 40 ns when it was bound to importin-β (Figure 6B). The unfolding transition proceeded from both termini as well as from kinks in the central section, which developed mainly at the intermittent negatively charged groups, such as Glu33 and Asp44/Asp45, with which the positive residues of the IBB center and termini started to form salt bridges. These negative residues are highly conserved in the IBB domain (Cingolani et al., 1999). The kinks are the starting points for unfolding,
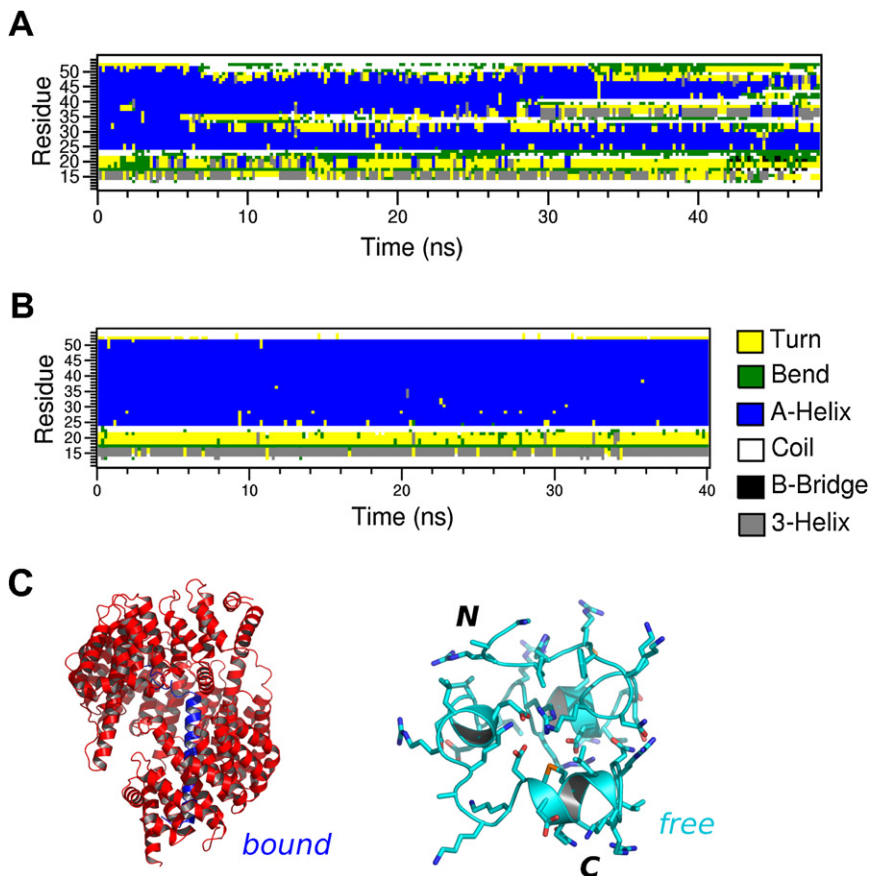
A

B

C

bound   *free*

Figure 6. Fast Unfolding of the IBB Domain
(A) Outside importin-β, the straight α-helical form of IBB rapidly unfolds, starting from kinks that develop around salt bridges at residues Glu33 and Asp45 (at t ≈ 6 ns and t ≈ 34 ns, respectively).
(B) Bound inside importin-β, the α helix of the highly basic domain remains completely stable.
(C) The α helix of the IBB domain (blue) in the bound state to importin-β (red), and after its collapse in the free state (cyan).

teins in the nucleus. Thus, we suggest that fast unfolding of the cargo adaptor, as shown above, plays a role in the classical nuclear import pathway involving importin-α.

DISCUSSION

Our simulations reveal a highly flexible and dynamic free importin-β structure, which undergoes large conformational changes and fluctuations. Its compact form, seen in the complexes bound to cargo (Cingolani et al., 1999; Lee et al., 2003), RanGTP (Lee et al., 2005), or the nucleoporin Nup1p (Liu and Stewart, 2005), can only be rigidified by strong binding of these molecules inside importin-β, thereby connecting the gap between the extremely flexible importin-β N and C termini and the rigid center. Free in solution, we propose a drastically extended S-like form of importin-β that exposes all binding sites to the cytoplasm. This geometry is consistent with its function in rapidly sequestering proteins destined for the nucleus (Stewart, 2007; Koerner et al., 2003), and also with its role as a chaperone, binding highly basic peptides in the cytoplasm to prevent their aggregation (Jäkel et al., 2002).

By contrast, the exportin CAS/Cse1p closes its superhelical conformation after RanGTP dissociates in the cytoplasm, thereby sealing off its binding sites and preventing RanGTP and importin-α from rebinding. By this mechanism, CAS ensures an efficient, one-way transition (Cook et al., 2005; Zachariae and Grubmüller, 2006). The fact that importin-β undergoes a transition to an extended state upon dissociation of its binding partners implies that rebinding of its partners is significantly favored over dissociation. As a consequence, the apparent affinities to RanGTP, the IBB domain, or Nup1p are very high (Bischoff and Görlich, 1999; Villa Braslavsky et al., 2000; Koerner et al., 2003; Pyhtila and Rexach, 2003; Figure 7A, right). The actual disassembly reaction may be accelerated due to the loaded spring character of importin-β. In order to furnish rapid, efficient transition from one complex into another and avoid close rebinding, a cooperative mechanism is necessary, because importin-β must be reliably converted into its compact state in order to seal off most of its binding surface. Interestingly, this explains why the IBB domain of importin-α is required to stimulate the dissociation of
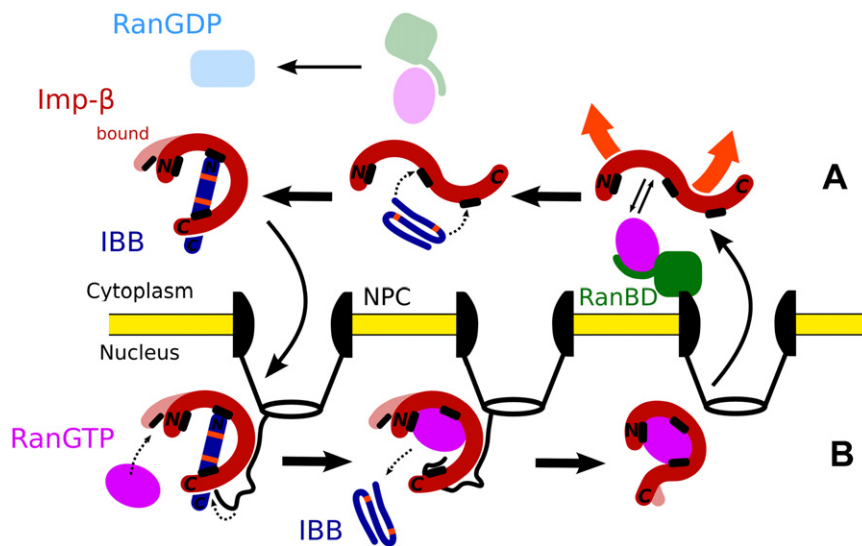
as they disrupt the straight α-helical form first. Subsequently, the regions between the kinks are gradually destabilized and lose their helical form (Figure 6A). Eventually, the free IBB domain collapses back upon itself, thereby hiding many of its binding sites from importin-β (Figure 6C).

On the side of the receptor, importin-β enters a fast transition into its extended state when the IBB domain is removed (Figure S4). This result shows that complexation mutually stabilizes the secondary structure of the IBB domain and the tertiary structure of importin-β.

These results explain the previous finding that double mutants, in which tryptophan groups from both termini of importin-β that are involved in binding the IBB domain were substituted by alanine (e.g., W342A/W864A), exhibit a drastically reduced affinity for the IBB domain (WT, ∼0.6 nM; W342A/W864A, ∼0.5 mM) (Koerner et al., 2003). Dissociation of the termini allows development of the central kinks, leading to unfolding of the helical IBB structure and, concomitantly, to an expansion of the importin-β conformation. The results demonstrate that importin-β has a chaperone function for highly basic peptides (Kobe, 1999; Catimel et al., 2001).

In the case of direct interaction with cargo, equivalent conclusions can be drawn with regard to importin-β (fast opening of importin-β after cargo removal; Figure S4). It is conceivable—but we consider it unlikely—that the four helices of SREBP-2 bound to importin-β undergo a similar unfolding reaction as that seen for the IBB domain, since they subsequently associate with pro-

Figure 7. Model of Spring-Assisted Facilitated Cargo and RanGTP Exchange of Importin-β and Protein Dynamics in the Nuclear Import Cycle

Importin-β is shown in red, the IBB domain in blue, RanGTP in magenta, and RanBD in green. ([A], right) RanBD binds to the importin-β-RanGTP complex and dissociates RanGTP. Dissociation releases the spring of importin-β, which opens up rapidly, exposing its acidic inner surface to the cytoplasm. ([A], center) Due to its open conformation, the IBB domain of importin-α can enter, bind, and reconstitute the compact, bound state of importin-β. In the absence of importin-α, reassociation with RanGTP is strongly favored. ([A], left) The formed import complex is translocated through the NPC. ([B], left) Approach of RanGTP to the N-terminal arch of importin-β in the nucleus. RanGTP initially binds to the N-terminal CRIME domain. ([B], center) Competition of RanGTP for the central IBB binding site, the acidic loop, and competition of Nup1 for the C-terminal IBB binding site releases the unfolding switch of the IBB domain (conserved intermittent acidic residues in the center [orange]). ([B], right) Full binding of RanGTP locks importin-β in a rigid conformation, except for HEAT repeats 17–19 at the far C terminus, and blocks its major IBB binding sites. IBB rebinding is hindered.

RanGTP from importin-β in the cytoplasm (Floer et al., 1997; Bischoff and Görlich, 1999). RanGTP is subsequently hydrolyzed to RanGDP by the RanGTPase-activating protein RanGAP, bound to RanBP (Ran binding protein), and RanGDP exhibits only very low affinity toward importin-β (Figure 7A, center/left).

On the other hand, a primary binding site for RanGTP is very accessible, even when the IBB domain is bound to importin-β in the nucleus. Here, we suggest a cooperative exchange mechanism, in which the unfolding of the IBB domain plays a major role (Figure 7B, center). In this sense, our results extend the zipper-like, allosteric exchange mechanism for IBB release in the nucleus proposed by Lee et al. (2005), and add atomic detail. According to the model, the partial opening of the N-terminal section in the cargo-bound states (Figure 4) would assist initial binding of the RanGTP switch II region to the CRIME domain (HEAT repeats 1–3) (Figures 3 and 7B, left). The observed intermittent closing motions (Figure S2) enable the basic patch of Ran to approach the acidic loop 8 of importin-β, where the N terminus of the IBB domain could then be displaced by active competition. Indeed, in our simulation, the acidic loop was drastically rigidified upon RanGTP binding (Figure S3), indicating a tighter interaction with RanGTP as compared with IBB.

The transition from the IBB-bound state to the RanGTP complex is kinetically fast, in spite of the high involved IBB binding affinity. This high affinity would suggest slow passive IBB dissociation, followed by reassociation of Ran. The N-terminal RanGTP binding site of importin-β, however, is accessible and open in our simulations. Its opening dynamics might facilitate RanGTP association in the nucleus. Our data also suggest that the C terminus of Nup1 may compete with the IBB domain for binding sites at the internal surface of importin-β.

We showed that dissociation from importin-β drives the transition of the IBB domain into its unfolded state (Figure 7B, center). This unfolding reaction is based upon the presence of intermittent, highly conserved acidic residues in the IBB domain, which do not interact with the strongly acidic binding channel of importin-β (Cingolani

et al., 1999), but serve as switches that rapidly disrupt the straight helical form of the IBB when dissociated. In that sense, Nup1 may assist RanGTP in unbinding importin-α from importin-β in the nucleus, in addition to its affinity to importin-α, which enhances the rate of nuclear import by accelerating cargo release from importin-α by competition (Pyhtila and Rexach, 2003). Cse1 and Nup2 then sequester importin-α and withdraw it from the equilibrium, accelerating this transition further (Stewart, 2007).

As the last step, binding of the RanGTP switch I region to HEAT repeats 13–15 locks the importin-β C terminus into its rigid conformation, which is incompatible with IBB rebinding (Lee et al., 2005). Our data showed that it blocks the conformational switch between HEAT repeats 14 and 15 (Figure 7B, right). The finding that the spring-loaded state of importin-β can store considerable energy suggests that the exchange of RanGTP or cargo is supported by partial relaxation (opening) of importin-β. Consistent with our suggestion, experiments have demonstrated that the Ran K37D/K152A mutant, which disrupts interaction of Ran with HEAT repeats 13 and 14, can accommodate binding of both RanGTP and the IBB domain (Lee et al., 2005).

Within a larger context, the highly flexible free structure of importin-β exhibits features of structural disorder. Although its secondary structure is well defined, its overall geometry is strongly influenced by the interaction with other proteins (Kobe and Kajava, 2000). This partial "tertiary disorder" enables importin-β to adapt its geometry to cargoes of different size and shape, and to RanGTP. Importin-β shares this feature with typical intrinsically unstructured proteins involved in molecular recognition, where a disorder-order transition, quite generally, is the key for combining binding specificity with reversibility by compensating binding energy with a decrease in entropy (Tompa, 2002; Dyson and Wright, 2005). Here, we have demonstrated that karyopherins combine this entropy-controlled mechanism with a second, enthalpy-dominated mechanism based on their well-defined secondary structure—the accumulation of significant strain between and within α-helical modules. In this sense, karyopherins

may be referred to as "semidisordered," and thus as a "missing link" between fully structured and fully disordered proteins. Being much more accessible to both experiment and simulation, semidisordered proteins might open a new route to elucidating entropy/enthalpy compensation and entropic strain as general functional principles of disordered proteins.

EXPERIMENTAL PROCEDURES

The available X-ray structures of the molecular complexes of yeast importin-β (Kap95p) bound to RanGTP (Lee et al., 2005; PDB code: 2BKU), importin-β bound to the IBB domain of importin-α (Cingolani et al., 1999; PDB code: 1QGK), importin β associated with the SREBP-2 (Lee et al., 2003; PDB code: 1UKL), and of Kap95p bound to the nucleoporin Nup1p (Liu and Stewart, 2005; PDB code: 2BPT) were taken from the protein data bank (PDB). The protonation states of titratable groups were determined with Whatif (Vriend, 1990) and its interface to DelPhi (Nicholls and Honig, 1991). Short missing loop sections, as well as missing side chains, were inserted and optimized with Whatif (Vriend, 1990). For the simulation of the unbound state, RanGTP or cargo were removed, respectively, from the protein complexes, and the void was refilled with water molecules. The structures were solvated in dodecahedral boxes with box vectors of ~14.3 nm length, with an ionic concentration corresponding to ~0.15 M. The systems were energy minimized, followed by relaxation for 400 ps, with positional restraints on the protein heavy atoms by using a force constant of $k = 1000$ kJ mol^{-1} nm^{-2}. The total system sizes varied between ~265,000 and ~300,000 atoms. Subsequently, trajectories of up to ~27 ns length were produced by free (unbiased) MD simulations. No explicit equilibration phase for the entire system was required for these intrinsically nonequilibrium simulations. A similar set-up was chosen for the simulations of the bound and unbound IBB domain of importin-α of up to 48 ns. All simulations were carried out with the MD software packages GROMACS 3.2.1 and 3.3 (van der Spoel et al., 2005). The OPLS-all atom force field (Jorgensen et al., 1996) was used for the protein, and TIP4P was used as the water model (Jorgensen et al., 1983). All simulations were performed in the NPT ensemble. The temperature was kept constant by Berendsen coupling at T = 310K, with a coupling time of $\tau_t = 0.1$ ps (Berendsen et al., 1984). The pressure was coupled to a Berendsen barostat with $\tau_p = 1.0$ ps and an isotropic compressibility of 4.5×10^{-5} bar^{-1} in the x, y, and z directions (Berendsen et al., 1984). All bonds were constrained with the LINCS algorithm (Hess et al., 1997). An integration time step of 2 fs was used. Lennard-Jones interactions were calculated with a cut-off of 10 Å. Electrostatic interactions were calculated explicitly at a distance smaller than 10 Å; long-range electrostatic interactions were calculated by particle-mesh Ewald summation, with a grid spacing of 0.12 nm and fourth-order B-spline interpolation. Structures were written out every 1 ps for subsequent analysis. For analysis of the hinge domain motions of Kap95p, the program DynDom was used (Hayward and Berendsen, 1998). PyMol (http://www.pymol.org) was used for all molecular representations and the mesh representation of the SAXS model. The mesh plot was obtained by representing bead positions fitted into the original SAXS data (Fukuhara et al., 2004) as Gaussian functions, with a width of 1 nm to approximate the experimental resolution and contouring at 33% maximum density. The atomic fluctuations in Figure S2 were compared after performing a sequence alignment with Whatif (Vriend, 1990). Interhelical angles were determined between the principal axes of the helices, derived from a principal components analysis of the helix C_α positions with locally written code. The strain released by the opening of importin-β was estimated by calculating the Stokes frictional energy needed to drag the HEAT repeats through the solvent over the observed distances within 27 ns, with force-probe "pulling" simulations of the HEAT repeats as a reference. The entropy gain in the free state of importin-β with respect to the RanGTP-bound state was estimated by the corrected quasiharmonic approximation (Schlitter, 1993).

SUPPLEMENTAL DATA

Supplemental Data include four additional figures and are available with this article online at http://www.structure.org/cgi/content/full/16/6/906/DC1/.

REFERENCES

Berendsen, H.J.C., Postma, J.P.M., van Gunsteren, W.F., Di Nola, A., and Haak, J.R. (1984). Molecular dynamics with coupling to an external bath. J. Chem. Phys. 81, 3684–3690.

Bischoff, F.R., and Görlich, D. (1999). RanBP1 is crucial for the release of RanGTP from importin β-related nuclear transport factors. FEBS Lett. 419, 249–254.

Cansizoglu, A.E., and Chook, Y.M. (2007). Conformational heterogeneity of karyopherin β2 is segmental. Structure 15, 1431–1441.

Catimel, B., Teh, T., Fontes, M.R., Jennings, I.G., Jans, D.A., Howlett, G.J., Nice, E.C., and Kobe, B. (2001). Biophysical characterization of interactions involving importin-α during nuclear import. J. Biol. Chem. 276, 34189–34198.

Chook, Y.M., and Blobel, G. (2001). Karyopherins and nuclear import. Curr. Opin. Struct. Biol. 11, 703–715.

Cingolani, G., Petosa, C., Weis, K., and Müller, C.W. (1999). Structure of importin-β bound to the IBB domain of importin-α. Nature 399, 221–229.

Conti, E., Müller, C.W., and Stewart, M. (2006). Karyopherin flexibility in nucleocytoplasmic transport. Curr. Opin. Struct. Biol. 16, 237–244.

Cook, A., Fernandez, E., Lindner, D., Ebert, J., Schlenstedt, G., and Conti, E. (2005). The structure of the nuclear export receptor Cse1 in its cytosolic state reveals a closed conformation incompatible with cargo binding. Mol. Cell 18, 355–367.

Cook, A., Bono, F., Jinek, M., and Conti, E. (2007). Structural biology of nucleocytoplasmic transport. Annu. Rev. Biochem. 76, 647–671.

Dyson, H.J., and Wright, P.E. (2005). Intrinsically unstructured proteins and their function. Nat. Rev. Mol. Cell Biol. 6, 197–208.

Eisenberg, D., and McLachlan, A.D. (1986). Solvation energy in protein folding and binding. Nature 319, 199–203.

Fahrenkrog, B., and Aebi, U. (2003). The nuclear pore complex: nucleocytoplasmic transport and beyond. Nat. Rev. Mol. Cell Biol. 4, 757–766.

Floer, M., Blobel, G., and Rexach, M. (1997). Disassembly of RanGTP-karyopherin β complex, an intermediate in nuclear protein import. J. Biol. Chem. 272, 19538–19546.

Fukuhara, N., Fernandez, E., Ebert, J., Conti, E., and Svergun, D. (2004). Conformational variability of nucleo-cytoplasmic transport factors. J. Biol. Chem. 279, 2176–2181.

Goody, R.S. (2003). The significance of the free energy of hydrolysis of GTP for signal-transducing and regulatory GTPases. Biophys. Chem. 100, 535–544.

Görlich, D., Seewald, M.J., and Ribbeck, K. (2003). Characterization of Ran-driven cargo transport and the RanGTPase system by kinetic measurements and computer simulation. EMBO J. 22, 1088–1100.

Harel, A., and Forbes, D.J. (2004). Importin β: conducting a much larger cellular symphony. Mol. Cell 16, 319–330.

Hayward, S., and Berendsen, H.J. (1998). Systematic analysis of domain motions in proteins from conformational change: new results on citrate synthase and T4 lysozyme. Proteins 30, 144–154.

Hess, B., Bekker, H., Berendsen, H.J.C., and Fraaije, J.G.E. (1997). LINCS: a linear constraint solver for molecular simulations. J. Comput. Chem. 18, 1463–1472.

Jäkel, S., Mingot, J.M., Schwarzmaier, P., Hartmann, E., and Görlich, D. (2002). Importins fulfil a dual function as nuclear import receptors and cytoplasmic chaperones for exposed basic domains. EMBO J. *21*, 377–386.

Jorgensen, W.L., Chandrasekhar, J., Madura, J.D., Impey, R.W., and Klein, M.L. (1983). Comparison of simple potential functions for simulating liquid water. J. Chem. Phys. *79*, 926–935.

Jorgensen, W.L., Maxwell, D.S., and Tirado-Rives, J. (1996). Development and testing of the OPLS-AA force field on conformational energetics and properties of organic liquids. J. Am. Chem. Soc. *118*, 11225–11236.

King, M.C., Lusk, C.P., and Blobel, G. (2006). Karyopherin-mediated import of integral inner nuclear membrane proteins. Nature *442*, 1003–1007.

Kobe, B. (1999). Autoinhibition by an internal nuclear localization signal revealed by the crystal structure of mammalian importin alpha. Nat. Struct. Biol. *6*, 388–397.

Kobe, B., and Kajava, A.V. (2000). When protein folding is simplified to protein coiling: the continuum of solenoid protein structures. Trends Biochem. Sci. *25*, 509–515.

Koerner, C., Guan, T., Gerace, L., and Cingolani, G. (2003). Synergy of silent and hot spot mutations in importin-β reveals a dynamic mechanism for recognition of a nuclear localization signal. J. Biol. Chem. *278*, 16216–16221.

Kutay, U., Izaurralde, E., Bischoff, F.R., Mattaj, I.M., and Görlich, D. (1997). Dominant-negative mutants of importin-β block multiple pathways of import and export through the nuclear pore complex. EMBO J. *16*, 1153–1163.

Lee, S.J., Imamoto, N., Sakai, H., Nakagawa, A., Kose, S., Koike, M., Yamamoto, M., Kumasaka, T., Yoneda, Y., and Tsukihara, T. (2000). The adoption of a twisted structure of importin-β is essential for the protein-protein interaction required for nuclear transport. J. Mol. Biol. *302*, 251–264.

Lee, S.J., Sekimoto, T., Yamashita, E., Nagoshi, E., Nakagawa, A., Imamoto, N., Yoshimura, M., Sakai, H., Chong, K.T., Tsukihara, T., et al. (2003). The structure of importin-β bound to SREBP-2: nuclear import of a transcription factor. Science *302*, 1571–1575.

Lee, S.J., Matsuura, Y., Liu, S.M., and Stewart, M. (2005). Structural basis for nuclear import complex dissociation by RanGTP. Nature *435*, 693–696.

Liu, S.M., and Stewart, M. (2005). Structural basis for the high affinity binding of nucleoporin Nup1p to the *Saccharomyces cerevisae* importin-β homologue Kap95p. J. Mol. Biol. *349*, 515–525.

Mosammaparast, N., and Pemberton, L.F. (2004). Karyopherins: from nuclear-transport mediators to nuclear-function regulators. Trends Cell Biol. *14*, 547–556.

Nicholls, A., and Honig, B. (1991). A rapid finite difference algorithm, utilizing successive over-relaxation to solve the Poisson-Boltzmann equation. J. Comput. Chem. *12*, 435–445.

Pace, C.N., Shirley, B.A., McNutt, M., and Gajiwala, K. (1996). Forces contributing to the conformational stability of proteins. FASEB J. *10*, 75–83.

Pyhtila, B., and Rexach, M. (2003). A gradient of affinity for the karyopherin Kap95p along the yeast nuclear pore complex. J. Biol. Chem. *278*, 42699–42709.

Ribbeck, K., and Görlich, D. (2001). Kinetic analysis of translocation through nuclear pore complexes. EMBO J. *20*, 1320–1330.

Schlitter, J. (1993). Estimation of absolute and relative entropies of macromolecules using the covariance matrix. Chem. Phys. Lett. *215*, 617–621.

Schreiber, G., and Fersht, A.R. (1995). Energetics of protein-protein interactions: analysis of the Barnase-Barstar interface by single mutations and double mutant cycles. J. Mol. Biol. *248*, 478–486.

Sotomayor, M., and Schulten, K. (2007). Single molecule experiments in vitro and in silico. Science *316*, 1144–1148.

Stewart, M. (2007). Molecular mechanism of the nuclear protein import cycle. Nat. Rev. Mol. Cell Biol. *8*, 195–208.

Svergun, D.I., Richard, S., Koch, M.H., Sayers, Z., Kuprin, S., and Zaccai, G. (1998). Protein hydration in solution: experimental observation by X-ray and neutron scattering. Proc. Natl. Acad. Sci. USA *95*, 2267–2272.

Tompa, P. (2002). Intrinsically unstructured proteins. Trends Biochem. Sci. *27*, 527–533.

Vallone, B., Miele, A.E., Vecchini, P., Chiancone, E., and Brunori, M. (1998). Free energy of burying hydrophobic residues in the interface between protein subunits. Proc. Natl. Acad. Sci. USA *95*, 6103–6107.

van der Spoel, D., Lindahl, E., Hess, B., Groenhof, G., Mark, A.E., and Berendsen, H.J.C. (2005). GROMACS: fast, flexible, and free. J. Comput. Chem. *26*, 1701–1718.

Vetter, I.R., Arndt, A., Kutay, U., Görlich, D., and Wittinghofer, A. (1999). Structural view of the Ran-importin-β interaction at 2.3 Å resolution. Cell *97*, 635–646.

Villa Braslavsky, C.I., Nowak, C., Görlich, D., Wittinghofer, A., and Kuhlmann, J. (2000). Different structural and kinetic requirements for the interaction of Ran with the Ran-binding domains from RanBP2 and importin-β. Biochemistry *39*, 11629–11639.

Vriend, G. (1990). WHAT IF: a molecular modeling and drug design program. J. Mol. Graph. *8*, 52–56.

Weis, K. (2003). Regulating access to the genome: nucleocytoplasmic transport throughout the cell cycle. Cell *112*, 441–451.

Zachariae, U., and Grubmüller, H. (2006). A highly strained nuclear conformation of the exportin Cse1p revealed by molecular dynamics simulations. Structure *14*, 1469–1478.